Energetics of Domain−Domain Interactions and Entropy Driven Association of β-Crystallins

Y. V. Sergeev,*,‡ J. F. Hejtmancik,‡ and P. T. Wingfield§

National Eye Institute and National Institute of Arthritis and Musculoskeletal and Skin Diseases, National Institutes of Health, Bethesda, Maryland 20982

Received April 17, 2003; Revised Manuscript Received November 12, 2003

ABSTRACT: β-Crystallins are major protein constituents of the mammalian lens, where their stability and association into higher order complexes are critical for lens clarity and refraction. They undergo modification as the lens ages, including cleavage of their terminal extensions. The energetics of βA3- and βB2-crystallin association was studied using site-directed mutagenesis and analytical ultracentrifugation. Recombinant (r) murine wild type βA3- and βB2-crystallins were modified by removal of either the N-terminal extension of βA3 (rβA3Ntr) or βB2 (rβB2Ntr), or both the N- and C-terminal extensions of βB2 (rβB2NCtr). The proteins were expressed in Sf9 insect cells or *Escherichia coli* and purified by gel-filtration and ion-exchange chromatography. All β-crystallins studied demonstrated fast reversible monomer−dimer equilibria over the temperature range studied (5−35 °C) with a tendency to form tighter dimers at higher temperatures. The N-terminal deletion of rβA3 (rβA3Ntr) significantly increases the enthalpy (+10.9 kcal/mol) and entropy (+40.7 cal/deg mol) of binding relative to unmodified protein. Removal of both N- and C-terminal extensions of rβB2 also increases these parameters but to a lesser degree. Deletion of the βB2-crystallin N-terminal extension alone (rβB2Ntr) gave almost no change relative to rβB2. The resultant net negative changes in the binding energy suggest that βA3- and βB2-crystallin association is entropically driven. The thermodynamic consequences of the loss of βA3-crystallin terminal extensions by in vivo proteolytic processing could increase their tendency to associate and so promote the formation of higher order associates in the aging and cataractous lens.

Crystallins are critical for lens transparency and refraction. Three major classes of ubiquitous crystallins are found in the vertebrate eye lens (*1*, *2*). The α-crystallins are related to the small heat-shock protein family (*3*). The β- and γ-crystallins form a superfamily of $\beta\gamma$-crystallins and share conserved sequences and a common fold of their polypeptide chains (*4*). $\beta\gamma$-Crystallins comprise two globular domains connected by an interdomain linker. Each domain is composed of two similar polypeptide chain motifs, forming two "Greek key" folds packed in a β-sandwich of two antiparallel β-sheets (*5*−*9*). Mutations in $\beta\gamma$-crystallin genes can lead to aggregation of protein and cataract formation (*10*−*19*).

Crystallographic studies show the two domains in γB- and βB2-crystallins adopt either a "closed" conformation in a monomer or an "open" one in a dimer, respectively (*20*). In both these conformations, similar surface areas form the interdomain interfaces (*9*, *21*). The surface residues forming the interface in βA3-crystallin (βA3) have similar physical properties to those in γB- and βB2-crystallin (*22*). Dimerization of two β-crystallin monomers is proposed to involve their transition from a closed to an open conformation followed by dimer formation (*23*). This model allows for a rapid interchange of monomers between β-crystallin complexes (*23*, *24*). The N- and C-terminal extensions of β-crystallins have extended conformations which have been suggested to modulate protein association (*25*). NMR data suggest that the N-terminal extension of bovine βA3 (residues 1−22) is flexible and solvent exposed (*26*). The binding energies predicted by the monomer−dimer equilibrium model agree with the energies determined from sedimentation equilibrium data at 20 °C for rβA3,[1] the N-terminal truncated mutant (rβA3tr), and an interdomain mutant in which the connecting linker is replaced by the corresponding sequence from γB-crystallin (rβA3cp, where "cp" refers to connecting peptide) (*23*). Murine βB2-crystallin also exhibits reversible monomer−dimer association (*24*) as do bovine βA3- and βB2-crystallins (*27*). Removal of residues at the N-terminus (residues 1−15) or the C-terminus (residues 175−185) does not appear to have a major effect on dimer formation or protein folding of bovine βB2-crystallin (*28*).

Study of truncated and mutant β-crystallins provides insight into the importance of specific structural domains for protein stability and association and, thus, into the molecular basis of cataract formation in both human and animal models. To investigate further the importance of

* Correspondence to Yuri V. Sergeev, OGVFB/NEI/NIH, 10/10B10, 9000 Rockville Pike, Bethesda, MD 20892. Tel: 301-594-7053. Fax: 301-435-1598. E-mail: sergeev@helix.nih.gov.

‡ National Eye Institute.

§ National Institute of Arthritis and Musculoskeletal and Skin Diseases.

[1] Abbreviations: An "r" preceding a crystalline name refers specifically to the recombinant protein, while the absence of an "r" refers to crystallins in general terms; DTT, dithiothreitol; EDTA, ethylendiaminetetraacetic acid; Tris, tris(hydroxymethyl) aminoethane; TCEP, tris(2-carboxyethyl) phosphine hydrochloride; SDS, sodium dodecyl sulfate.

10.1021/bi034617f
Published on Web 12/18/2003

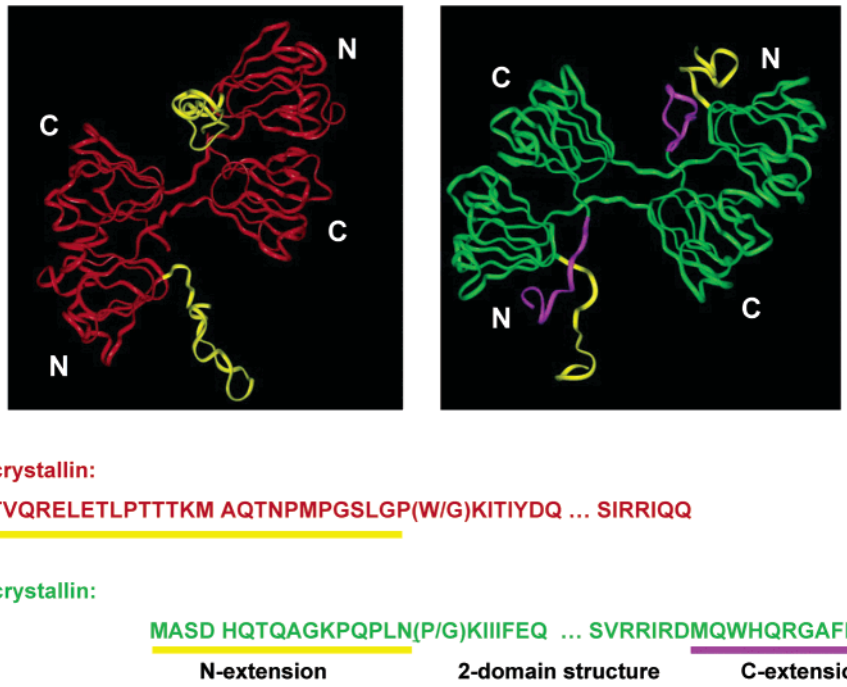

FIGURE 1: Three-dimensional structures and corresponding protein sequences showing structural domains deleted in wild-type proteins to create rβA3Ntr, rβB2Ntr, and rβB2NCtr. The structures of rβA3 and rβB2 were obtained by homology modeling similar as described (*23*) and their ribbon structures are shown by red and green, respectively (top panels). Yellow and violet show structures of the N- and C-terminal extensions, respectively. The N and C labels identify the N- and C-termini of the globular domains, respectively. Amino acid sequences with central parts not shown are shown in red (rβA3) and green (rβB2). Deleted sequences in truncated proteins rβA3Ntr and rβB2NCtr are underlined in the same colors as described above. Symbols in parentheses (W, P/G) show mutation from residue Trp or Pro to residue Gly.

domain−domain interactions and terminal extensions for dimerization of β-crystallin, the energetics of the self-association of wild-type rβA3 and rβB2 crystallins were studied and compared to truncated variants in which the N-terminal extensions (rβA3Ntr or rβB2Ntr), or both N- and C-terminal extensions (rβB2NCtr) were removed (Figure 1). All recombinant βA3 and βB2 proteins appear to conform to a reversible monomer−dimer equilibrium system. In general, βA3- and βB2-crystallins both tend to form tighter dimers with increasing temperatures. Negative changes in the binding energies resulted from positive changes in enthalpy and entropy, which indicate that the associations are entropically driven. Thus, the loss of amino-terminal extensions increases the propensity of the βA3- and βB2-crystallins to dimerize by increasing the entropy of association. This may have physiological importance if proteolytic processing in vivo results in removal of the terminal extensions because it would increase the potential for protein association, which in turn could influence lens aging and cataractogenesis.

MATERIALS AND METHODS

Cloning and Expression. Wild type and mutant recombinant murine rβA3-crystallins were expressed in baculovirus as previously described (*29*, *30*). In rβA3Ntr, N-terminal residues 1−29 were deleted and residue 30 was replaced by glycine (W30G). Recombinant murine rβB2 crystallin and the N-terminal deletion mutant rβB2Ntr, with residues 1−16 deleted and residue 17 replaced by glycine (P17G), were constructed as previously described (*31*). Both truncated crystallins, thus, have the same N-terminus as γB-crystallin. This allows for direct comparison of the domain interactions of the truncated β-crystallins and γ-crystallins. Furthermore, the substitution may also prevent nonphysiological aggregation that can result from inadvertent exposure of a novel amino acid to the surface of the molecule (*32*). The C-terminal residues 173−185 of rβB2NCtr were deleted by PCR-mutagenesis of the transfer plasmid pBBβB2Ntr to create the recombinant vector pBBβB2NCtr. To confirm that pBBβB2NCtr was in the correct orientation and contained the correct sequence, restriction enzyme mapping (KphI, PvuII, HindIII, and BglII) and bidirectional sequencing using the dideoxy chain termination method (fmol DNA Sequencing System, Promega, Madison, WI) were performed. Hence, rβB2NCtr has the following modifications: N-terminal deletion residues 1−16; mutation P17G, and C-terminal deletion, residues 173−185. The double deletion construct pBBβB2NCtr was cotransfected with wild-type AcMNPV DNA into Sf9 insect cells followed by plaque purification of recombinant (gal+, occ-) virus. Eight pure recombinant clones were screened for relative protein expression levels. The two clones expressing at the highest levels were selected for use in protein expression. The cDNA coding for rβB2-crystallin was amplified using PCR primers containing NdeI and XhoI sites and was cloned into the NdeI and XhoI sites in pET-20b(+) vector (Novagen, Madison, WI) (kind gift of Dr. H. Mchaourab). Protein was expressed in BL21(DE3) cells according to standard procedures (Novagen, Madison, WI).

Protein Purification. The rβA3 and rβB2 crystallins and corresponding variants were purified using the same method. Briefly, infected insect cells were lysed by freeze−thawing in 1 mL of buffer A: 50 mM Tris-HCl, pH 7.5, 1 mM EDTA, and 1 mM DTT. *Escherichia coli* infected cells were

sonicated on ice (+4 °C) instead of the freeze−thawing step. All lysates were centrifuged at 10600*g* for 30 min at 4 °C, and the supernatants were dialyzed overnight against 1 L of buffer A containing 1 μM E-64 Cys protease inhibitor (Boehringer Manniheim GmbH, Indianapolis, IN). Proteins were purified at room temperature using a FPLC Bio-Logic Duo-Flow workstation (Bio-Rad, Hercules, CA). Soluble extracts were loaded on a 1.6-cm × 60-cm (120 mL) HiPrep 16/60 Sephacryl S-200 High-Resolution column (Amersham Biosciences, Piscataway, NJ) equilibrated with buffer A and eluted at a flow rate of 0.5 mL/min; 2.5 mL fractions were collected. Fractions containing recombinant proteins (see below) were dialyzed against either buffer B: 50 mM Tris-HCl, pH 8.5, 1 mM EDTA, 1 mM DTT (rβA3 proteins) or buffer C: 20 mM Tris-HCl, pH 8.5, 1 mM EDTA, 1 mM DTT (rβB2 proteins). To obtain protein with > 95% purity, it was sometimes necessary to perform further purification by ion-exchange chromatography using a 5 mL Hi-Trap DEAE-10 column equilibrated with buffer B (rβA3) or buffer C (rβB2). Proteins (5 mL) were loaded on the column at a flow rate of 0.5 mL/min, a 0−1 M NaCl salt gradient was applied and 2.5 mL fractions were collected.

The location of recombinant proteins in column fractions was monitored by absorbance at 280 nm and by SDS−PAGE using 12% polyacrylamide gels (*33*). Protein identity was confirmed by Western blot analysis using rabbit antisera against a synthetic peptide corresponding to residues 36−68 of murine βA3-crystallin or against residues 1−11 of βB2-crystallin (*34*). In some cases, we also used rabbit anti-β-crystallin antibodies, kindly provided by Dr. S. Zigler (NEI/NIH). The masses of proteins purified from *E. coli* were determined by mass spectrometry and corresponded to that predicted from the respective gene sequences minus the initiating methionines.

Gel-Filtration Chromatography. Analytical gel-filtration was performed using a 1-cm × 30-cm (24 mL) Superdex-75 HR 10/30 column (Amersham Biosciences, Piscataway, NJ) equilibrated in buffer D: 50 mM Tris-HCl, pH 7.5, 1 mM EDTA, 1 mM DTT, 150 mM NaCl, and 50 μM TCEP. The flow rate was 0.5 mL/min and 0.5 mL fractions were collected. The column was precalibrated with low-molecular weight standards: bovine serum albumin, ovalbumin, carbonic anhydrase, chymotrypsinogen, cytochrome *c*, ribonuclease A and aprotinin (Amersham Biosciences, Piscataway, NJ; Sigma-Aldrich Inc, St. Louis, MO). The void and included volumes of the column were determined with Blue Dextran 2000 and 20% acetone, respectively.

Analytical Ultracentrifugation. Only samples showing a single peak on analytical gel-filtration columns and which were greater than 95% pure as judged by SDS−PAGE were used for analytical ultracentrifugation. To minimize artifactual association of proteins due to sulfhydryl oxidation, samples (10 μM) were incubated for 1 h at room temperature in buffer D containing 10 mM DTT and 1.5 M urea, followed by dialysis for 24 h at 4 °C against of 1 L of buffer D. Prior to a centrifugation, 50 μM of the reductant, Tris[2-carboxyethyl]-phosphine (TCEP; Pierce Biotechnology Inc., Rockford, IL) was added to the proteins and reference buffer.

Centrifugation was carried out using a Beckman Optima XL-I analytical ultracentrifuge (*35*). Absorption optics, an An-60 Ti rotor, and standard double-sector centerpiece cells were used. All analyses were performed using duplicate protein samples. Prior to the temperature dependence studies, proteins were prescreened at 20 °C; data were collected after 16−20 h at 16 500 rpm and baselines established by overspeeding at 45 000 rpm for a further 4 h. Equilibria profiles (the average of five scans using a radial step size of 0.001 cm) were analyzed using standard Optima XL-I Origin-based data analysis software. The parameters used in data analysis, including molecular weight (M_r), partial specific volume and molar extinction coefficient, are shown in Table 1. Solvent density was estimated as previously described (*36*). Monomeric molecular weights and molar extinction coefficients indicated in Table 1 were used for calculation of dissociation constants (K_d). Variation of partial specific volume and solvent density with temperature was also determined according to ref *36*.

Table 1: Parameters Used, Sedimentation Equilibrium, and Gel-Filtration Data Obtained for Wild Type and Mutant Recombinant β-Crystallins at 20 °C[a]

	calculated parameters			gel-filtration	sedimentation equilibrium	
protein	M_r kDa	ρ mL/g	ϵ mM^{-1} cm^{-1}	M_r, kDa	M_r kDa	K_d M
rβA3	25.1	0.717	63.19	40	42.6 (±0.7)	5.1 (±0.7)
rβA3Ntr	21.8	0.715	57.64	23	42.7 (±0.1)	0.7 (±0.1)
rβB2	23.3	0.720	38.40	37	37.6 (±0.2)	4.6 (±1.1)
rβB2Ntr	21.6	0.721	38.60	36	34.5 (±0.8)	9.67 (±3.0)
rβB2NCtr	20.1	0.723	33.02	28	34.9 (±0.5)	4.9 (±1.6)

[a] Molecular weight (M_r) and partial specific volume ρ (*59*) were calculated from protein sequences. For all proteins, the initiating N-terminal methionine had been processed. Apparent molecular weights (M_r) were determined by gel-filtration. They are intermediate between the monomer and dimer molecular weights and presumably represent either a rapid equilibrium between two states or perhaps some equilibrium interaction between protein and gel matrix. Both dissociation constants (K_d) and weighted-average molecular weight (M_r) were determined from sedimentation equilibrium using a monomer−dimer equilibrium model fitting concentration profiles as previously described (*23*). For the calculation of dissociation constants molecular weights of monomers and molar extinction coefficients ϵ were used. Presented values M_r and K_d were averaged over repeated experiments for different samples of the same protein at 20 °C. Standard root-mean square errors (rms) demonstrating variability between samples of same protein are shown by values in parentheses.

Monomer−dimer equilibrium was measured at temperatures between 5 and 35 °C as it is expected that there should be no unfolding or aggregation of protein over this temperature range. Measurements were performed using 5 °C step intervals as follows: wild-type rβA3 and rβB2 were measured in two overlapping temperature ranges of 5−25 and 15−35 °C. The same protein sample was used for all measurements within each temperature range. This procedure, which is made possible by the use of the strong reducing agent TCEP, allows equilibrium measurements to be made with significantly less protein compared to methods currently used for analytical ultracentrifugation studies at varying temperatures (*42*). For the modified crystallins rβA3Ntr, rβB2Ntr, and rβB2NCtr, temperature ranges of 5−25 °C (rβA3Ntr) or of 5−20 °C (rβB2Ntr and rβB2NCtr) were used. Data were collected by first establishing equilibrium (~16 h at 16 500 rpm) at the lowest temperature in the range (often 5 °C), the temperature was then raised 5 °C, and measurements were taken 8 h later (scans from 4 to 8 h were used to confirm equilibrium status). After the

final (highest) temperature data set had been recorded, overspeeding at 45 000 rpm was used to establish a baseline (the temperature was reset to 20 °C for this measurement).

Dissociation constants were determined by fitting a monomer−dimer equilibrium model to the concentration gradients established at each temperature. Average dissociation constants were determined by averaging two sets of dissociation constants collected from duplicate samples at a given temperature. For wild-type proteins, the two datasets corresponding to overlapping temperature ranges were multiplied by scale coefficients determined from the average of the dissociation constants. This procedure helped to correct inaccuracies in the baseline determination.

Energetics of Monomer−Dimer Equilibrium. The temperature dependence of the dissociation constants for wild-type proteins was used to determine thermodynamic parameters for the reversible monomer−dimer association, by fitting the nonlinear function (*37*) into the set of experimental dissociation constants determined at different temperatures

$$\ln(K_d(\mathrm{wt})/C_o) = (1/R)[\Delta C_p(293.15/T - \ln(293.15/T) - 1) - \Delta H_d^\circ/T + \Delta S_d^\circ] \quad (1)$$

where T is the temperature (K), C_o is the molar concentration of protein in μM, ΔH_d° and ΔS_d° are changes in enthalpy and entropy due to dissociation, and ΔC_p is the change in protein heat capacity in the standard state. Fitting was repeated in two different ways for each wild-type protein. First, ΔC_p was constrained to be zero, and second, no constraints were imposed and changes in enthalpy and entropy (ΔH_d° and ΔS_d°), including possibly nonzero values of ΔC_p, were determined. Calculations of thermodynamic parameters were duplicated only for wild-type proteins because of the larger number of independent measurements (seven) in the temperature range from 5 to 35 °C as compared to four for the truncated variants. For these proteins, both linear and nonlinear fits are qualitatively similar, and the relatively small values of ΔC_p (−0.9 and 0.7 cal/deg mol, Table 4) with an error of 0.5−0.6 cal/deg mol suggest that the data for truncated variants can be calculated using the linear method.

The effect of removing the terminal extension on the equilibrium between monomer and dimer can be estimated using

$$\Delta\Delta G_d = -RT \ln(K_d(\mathrm{trunc})/K_d(\mathrm{wt})) \quad (2)$$

where K_d(trunc) and K_d(wt) are dissociation constants measured for truncated and wild-type protein, respectively. Changes in the thermodynamic parameters due to removal of terminal extensions were calculated by fitting the following linear function to the plot of $\ln(K_d(\mathrm{trunc})/K_d(\mathrm{wt}))$ versus $1/T$ derived from the observed experimental data

$$\ln(K_d(\mathrm{trunc})/K_d(\mathrm{wt})) = -(\Delta\Delta H_d^\circ/R)\ 1/T + \Delta\Delta S_d^\circ/R \quad (3)$$

where $\Delta\Delta H_d^\circ$ and $\Delta\Delta S_d^\circ$ are the standard enthalpy and entropy changes due to the mutation.

RESULTS

Monomer−Dimer Equilibrium at 20 °C. The expression and purification of rβB2 from *E. coli* or insect cells results in proteins that are chemically (using mass spectrometry and SDS−PAGE), conformationally (using far-UV circular dichroism), and physically (using analytical ultracentrifugation and gel filtration) indistinguishable from one another. Recombinant βA3- and βB2-crystallins produced in sf9 cells are also similar to naturally occurring mouse lens β-crystallins in terms of SDS−PAGE, far-UV circular dichroism, and gel-filtration chromatography. In addition, when mixed with naturally occurring mouse β-crystallins, they were incorporated into βH and βL associates similarly as assessed by sieve gel chromatography (*30*). However, in this study we used the *E. coli* derived protein because of superior expression and purification yields compared to the baculovirus system.

The native molecular weights of wild type and truncated β-crystallins were determined using sedimentation equilibrium at 20 °C (Table 1). The molecular weights determined were intermediate between the monomer and dimer weights, and a monomer−dimer model was applied to the analyses of the equilibrium concentration profiles (Figure 2 A−E). The residuals from the model scatter randomly around the zero value for rβB2Ntr and rβB2NCtr (Figure 2E,D), whereas for rβA3, rβB2, and mutant rβA3Ntr there is a slight systematic trend with negative errors near the bottom of the cell (Figure 2A−C). This is most likely due to the presence of small amounts (<5%) of higher order irreversible aggregates. Other models, for example, monomer−trimer and monomer−tetramer, were tested to check for better fits than the monomer−dimer model (lower χ^2-statistics), and all produced significantly worse fits. These results are similar to those previously described for rβA3 and rβA3Ntr (*23*).

The K_d's for wild-type rβA3 and the N-terminal truncated variant rβA3Ntr were estimated as 5.1 and 0.7 μM, respectively (Table 1; Figure 2A,B). The lower K_d of the truncated protein indicates tighter dimer formation, for example, at 1 mg/mL, ∼92% is dimeric compared to 78% of the intact protein. The K_d data obtained at 20 °C for both proteins are both close to the K_d data published earlier (*23*). The equilibrium constants for rβB2 and rβB2NCtr were fairly similar, 4.6 and 4.9 μM, respectively (Table 1; Figure 2C,D). At 1 mg/mL, approximately 80% of both rβB2 and rβB2NCtr are predicted to be dimeric. The equilibrium constant calculated for rβB2Ntr is 9.7 μM, showing that rβB2Ntr is a less stable dimer compared to the wild-type protein and the double truncated mutant (Table 1, Figure 2E). On the basis of the determined K_d values, the dimerization potential of rβA3Ntr is higher than that of rβB2NCtr despite the fact that both these N- and C-truncated proteins have similar two-domain structures.

The apparent molecular weights determined using Superdex-75 gel filtration (Table 1) agree with the centrifugation data except for rβA3Ntr, which elutes with an apparent molecular mass of 23 kDa, similar to that expected for a monomer. This anomaly, probably, due to interactions of rβA3Ntr with the gel matrix, has been previously discussed for βA3- and βB1-crystallins (*23*, *38*, *39*). The lower than expected molecular mass for rβB2NCtr (28 kDa) also suggests possible gel matrix interaction.

All experiments on monomer−dimer equilibrium were performed under reducing conditions. Indeed, obtaining consistent molecular weights for β-crystallins can be problematical, especially when using sedimentation equilibrium, because of the potential for intermolecular disulfide bond

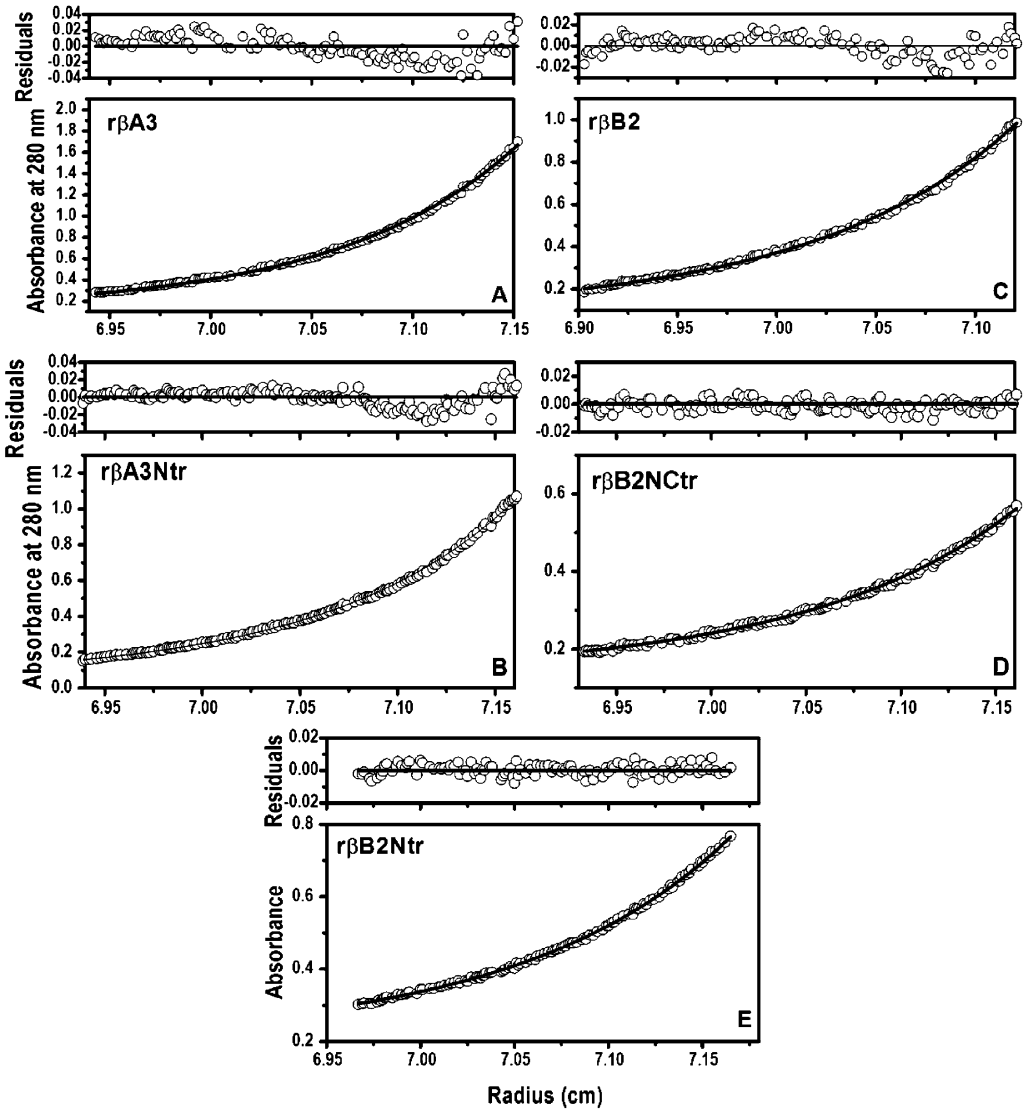

FIGURE 2: Sedimentation equilibrium data obtained for wild type and mutant rβA3- and rβB2-crystallins at room temperature (20 °C). Panels A are absorbance (bottom panel) and residuals (upper panel) plots for rβA3, panels B−E are the same data plots for rβA3Ntr, rβB2, rβB2NCtr, and rβB2Ntr, respectively. Opened circles show the protein concentration profile represented by the UV absorbance gradients in the centrifuge cell at 280 nm. The solid lines indicate the calculated fit for monomer−dimer association. Residuals in the top panels show the difference in the fitted and experimental values as function of radial position. The χ^2-statistics for the fits shown are 3.4×10^{-5}, 5.2×10^{-5}, 4.9×10^{-5}, 3.2×10^{-5}, and 1.06×10^{-5} for rβA3, rβA3Ntr, rβB2, rβB2NCtr, and rβB2Ntr, respectively. The dissociation constants (K_d) and weighted-average molecular weight (M_r) calculated from these plots are shown in Table 1.

formation by unpaired cysteines. This is especially true considering the long times involved in data collection (>24 h). Hence, in samples not carefully reduced as described (Material and Methods), it is common to see weight average molecular weights greater than that of the dimeric protein (*23*, *40*). For example, using rβB2 and rβB2NCtr, weight-average molecular weights determined in the presence of DTT were typically ~48 and ~50 kDa, respectively. Furthermore, the oxidation of DTT generates absorbance in the 280 nm range complicating baseline-offset determinations, a critical step in obtaining reliable molecular weight estimates. To prevent such artifacts, we have used the recently introduced reducing agent TCEP, which is a stronger reductant than DTT and allows for more reliable baseline estimations and, hence, molecular weight determinations (see Table 1).

Temperature Dependence of Monomer−Dimer Equilibrium. Tables 2 and 3 summarize the equilibrium constants determined for wild type and mutant crystallins as a function of temperature and also show the corresponding Gibbs free energy changes. For most of the β-crystallins studied, there is a reciprocal relationship between K_d and temperature; dimerization tends to increase (shown by a lowering of the K_d) as the temperature increases. This is also reflected by the increasingly negative free energy of association, ΔG_a, at higher temperatures. At each temperature the truncated crystallin variants bind (associate) more tightly than the corresponding native proteins, as indicated by higher (more negative) values of $\Delta\Delta G_a$. Over the temperature range studied, this trend is most clearly observed for rβA3Ntr, for which $\Delta\Delta G_a$ values are increasingly negative with increasing temperature. Although the trend is less apparent for rβB2NCtr and rβB2Ntr (Tables 2 and 3), all values of $\Delta\Delta G_a$ remain negative (rβB2NCtr) or positive (rβB2Ntr) over the temperature range studied.

The effects of temperature on the association constant are also shown by the Van't Hoff plots, where the natural logarithm of the K_d for the wild type is plotted against the

Table 2: Thermodynamic Data Obtained for the Dimerization of Recombinant Wild Type and Modified rβA3-Crystallins[a]

	K_d μM		ΔG_a kcal/mol		$\Delta\Delta G_a$ kcal/mol
T °C	*rβA3*	*rβA3Ntr*	*rβA3*	*rβA3Ntr*	*rβA3Ntr*
5	3.0(±0.6)	1.5(±0.7)	−0.7(±0.1)	−1.0(±0.3)	−0.3(±0.3)
10	1.5(±0.4)	0.3(±0.3)	−1.1(±0.1)	−1.8(±0.5)	−0.7(±0.5)
15	1.8(±0.7)	0.6(±0.3)	−1.0(±0.2)	−1.6 (±0.3)	−0.6(±0.4)
20	3.0(±1.2)	0.4(±0.6)	−0.7(±0.2)	−1.8(±0.8)	−1.1(±0.8)
25	2.0(±1.2)	0.2(±0.5)	−1.0(±0.4)	−2.2(±1.4)	−1.2(±1.4)
30	0.8(±0.9)		−1.5(±0.7)		
35	0.6(±0.8)		−1.8(±0.9)		

[a] Dissociation constants (K_d) were obtained as described in Materials and Methods using a global fit procedure. Standard errors were estimated from these data and are shown in parentheses. Gibbs free energy change for dimer association (ΔG_a) estimated as $\Delta G_a = -\Delta G_d$, where the dissociation free energy change is $\Delta G_d = -RT \ln(K_d/C_o)$. Here K_d is the dissociation constant and C_o is the protein sample concentration in μM. Values in the last column were calculated as $\Delta\Delta G_a = \Delta G_a(\text{trunc}) - \Delta G_a(\text{wt})$.

reciprocal of the absolute temperature (Figure 3A). The difference in heat capacity ΔC_p relates to changes in the internal structure of the proteins and surrounding water shell under heat application. This value, defined as the variation of enthalpy with temperature, can be determined from the Van't Hoff plot. The experimental data for wild-type proteins rβA3 and rβB2 were fitted twice using two separate functions. In the first ΔC_p is constrained to be 0, resulting in a linear function in which the entropy change can be obtained from the intercept and the enthalpy change from the slope of the Van't Hoff plot. The second, in which ΔC_p is not constrained, is a nonlinear function (eq 1 in Materials Methods). The results obtained using these fits are represented in Table 4. Dimerization of rβA3 is associated with positive enthalpy, $\Delta H_a = 7.2 \pm 3.0$ kcal/mol, and entropy, $\Delta S_a = 28.3 \pm 10.1$ e.u. changes (Table 4). The corresponding to thermodynamic parameters for association of rβB2 were $\Delta H_a = 4.0 \pm 2.3$ kcal/mol, and $\Delta S_a = 16.6 \pm 7.9$ e.u., are also both positive. For the nonlinear fit (i.e., ΔC_p is nonzero) the values of the enthalpy and entropy of dissociation are close to those expected assuming $\Delta C_p = 0$. Thus, the results of both linear and nonlinear fits indicate that the enthalpy and the entropy of association are higher for rβA3 than for rβB2. The flexibility and length of the βA3 amino-terminal extension might potentially contribute to the higher entropy change.

The energetic effect of the deletion of terminal extensions is shown in Figure 3B, in which the ratio $K_d(\text{trunc})/K_d(\text{wt})$ is plotted against the reciprocal of the absolute temperature (K). Values of $\Delta\Delta H_a^\circ$ and $\Delta\Delta S_a^\circ$ were estimated by a linear fit, assuming that the change of heat capacity for the deletion mutants is zero. Net changes in enthalpy and entropy for rβA3Ntr and rβB2NCtr are shown in Table 4. Removal of the amino-terminal extension of rβA3 increases the enthalpy of binding in the dimer by $\Delta\Delta H_a = 10.9 \pm 3.2$ kcal/mol and also increases entropy of dimerization by $\Delta\Delta S_a = 40.7 \pm 11.1$ e.u., resulting in negative change of association energy (−2 kcal/mol at 20 °C) as shown in Table 4 for rβA3Ntr. The enthalpy and entropy changes observed when both terminal extensions of rβB2 are removed (rβB2NCtr) are less significant ($\Delta\Delta H_a = 7.0 \pm 0.7$ kcal/mol and $\Delta\Delta S_a = 23.4 \pm 2.6$ e.u., respectively) and the energy of association (−0.7 kcal/mol) is also lower. Amino-terminal truncated mutant (rβB2Ntr) shows no change in binding enthalpy ($\Delta\Delta H_a \sim 0$) and only a small change in entropy of

Table 3: Thermodynamic Data Obtained for the Dimerization of Wild Type and Modified rβB2[a]

	K_d, μM			ΔG_a, kcal/mol			$\Delta\Delta G_a$, kcal/mol	
T °C	rβB2	rβB2Ntr	rβB2NCtr	rβB2	rβB2Ntr	rβB2NCtr	rβB2Ntr	rβB2NCtr
5	6.9(±1.9)	5.1(±1.7)	3.1(±1.7)	−0.3(±0.2)	−0.7(±0.2)	−0.9(±0.3)	−0.4 (±0.3)	−0.6(±0.4)
10	2.9(±1.0)	5.0(±1.6)	1.7(±1.2)	−0.8(±0.2)	−0.7(±0.2)	−1.3(±0.4)	0.1 (±0.3)	−0.5(±0.5)
15	1.9(±0.6)	5.4(±2.1)	1.3(±1.2)	−1.0(±0.2)	−0.6 (±0.3)	−1.5(±0.6)	0.4 (±0.4)	−0.5(±0.6)
20	2.5 (±0.8)	5.2 (±1.9)	2.3(±1.7)	−0.9(±0.2)	−0.7(±0.2)	−1.1(±0.5)	0.2 (±0.3)	−0.2(±0.5)
25	3.3(±0.9)			−0.8(±0.2)				
30	2.6(±0.8)			−0.9(±0.2)				
35	2.2(±1.8)			−1.0(±0.6)				

[a] Dissociation constants (K_d) were obtained as described in Materials and Methods using a global fit procedure. Standard errors were estimated from these data and are shown in parentheses. Gibbs free energy change for dimer association (ΔG_a) estimated as $\Delta G_a = -\Delta G_d$, where the dissociation free energy change is $\Delta G_d = -RT \ln(K_d/C_o)$. Here K_d is the dissociation constant and C_o is the protein sample concentration in μM. Values in the last column were calculated as $\Delta\Delta G_a = \Delta G_a(\text{trunc}) - \Delta G_a(\text{wt})$.

Table 4: Thermodynamic Parameter Changes Obtained for Wild Type and Truncated Crystallins[a]

protein	ΔH_a, kcal/mol	$-T\Delta S_a$, kcal/mol	ΔS_a, e.u.	ΔC_p, cal/deg mol	ΔG_a, kcal/mol
rβA3	7.9(±2.8)[b]	−8.9(±2.8)	30.4(±9.4)[b]	−0.9(±0.6)[b]	−1.0(±4.0)
	7.2(±3.0)	−8.4(±3.0)	28.3(±10.1)	0	−1.2(±4.2)
rβA3Ntr	18.8(±4.4)	−20.8(±4.3)	71.1(±14.5)	0	−2.0(±5.2)
rβB2	3.4(±2.1)[b]	−4.3(±2.0)	14.8(±7.1)[b]	0.7(±0.5)[b]	−0.9(±3.0)
	4.0(±2.3)	−4.9(±2.3)	16.6(±7.9)	0	−0.9(±3.3)
rβB2Ntr	4.1(±2.3)	−5.4(±4.8)	18.8(±16.3)	0	−1.3(±0.3)
rβB2NCtr	11.0(±2.4)	−11.7(±1.0)	40.0(±3.5)	0	−0.7(±2.6)

[a] Changes in enthalpy ΔH_a and entropy ΔS_a of wild-type proteins were determined by fitting functions (1) and (2) into van't Hoff plots (Figure 3A). Changes $\Delta H_a(\text{trunc})$ and $\Delta S_a(\text{trunc})$ for truncated proteins were calculated as sums of those for normal proteins plus values of $\Delta\Delta H_a$ and $\Delta\Delta S_a$, respectively: $\Delta H_a(\text{trunc}) = \Delta H_a(\text{wt}) + \Delta\Delta H_a$ and $\Delta S_a(\text{trunc}) = \Delta S_a(\text{wt}) + \Delta\Delta S_a$. Values of $\Delta\Delta H_a$ and $\Delta\Delta S_a$ were determined from Figure 3 as described in Materials and Methods. The Gibbs free energy change ΔG_a was calculated from these parameters by the formula $\Delta G_a = \Delta H_a - T\Delta S_a$. All parameters were determined with reference to the standard state (20 °C). Changes of entropy indicated in e.u. units: 1 e.u. = 1 cal/(deg mol). [b] Parameters determined using nonlinear fit procedure (nonzero ΔC_p).

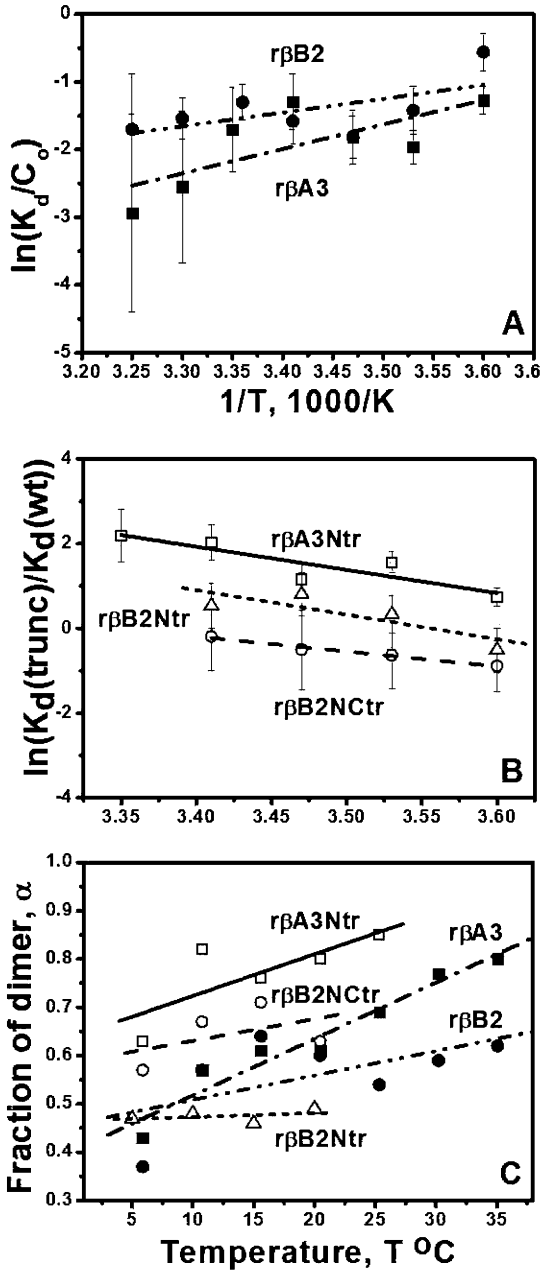

FIGURE 3: Graphic presentations of (A,B) the van't Hoff plot and (C) dimer fractions of wild type and truncated β-crystallins. van't Hoff plots of $\ln(K_d/C_o)$ (A) and of $\ln(K_d(\text{trunc})/K_d(\text{wt}))$ (B) as functions of the reciprocal absolute temperature (1000/K) are shown, where K_d's are the dissociation constants for wild type (wt) and truncated (trunc) proteins, and C_o is the molar concentration. Thermodynamic data are presented in Tables 2−4. Solid squares (dash−dot line) and circles (dash−dot−dot line) show data for rβA3 and rβB2, respectively. Opened squares (solid line), circles (dash line), and triangles (short dash line) correspond to data for rβA3Ntr, rβB2NCtr, and rβB2Ntr. Lines represent the result of linear fitting by the least-squares method.

association ($\Delta\Delta S_a = 2.2$ e.u.) resulting in an overall negative association energy change (−1.3 kcal/mol). The above determinations clearly indicate that removal of the terminal extensions of either rβA3 or rβB2 increases their dimerization potential with rβA3Ntr forming a stronger dimer than rβB2NCtr, or especially rβB2Ntr.

DISCUSSION

Monomer−Dimer Equilibrium. Sedimentation equilibrium determination of K_d values over a broad temperature range indicates the reversible dimerization of β-crystallins and their terminal deletion variants. The physical behavior of the crystallins appears to be independent of the particular method used for protein purification and the method used to study the native molecular weight (*23*, *24*, *26*). Structural models of monomers and dimers proposed to be involved in the equilibria are shown in Figure 4 with a schematic representation of the energetics (data from Tables 2 and 3 and (*23*)) of subunit exchange. In this scheme, monomers in a "closed" conformation are in equilibrium with dimers having an "open" conformation via an energetically unfavored monomer intermediate in an open conformation. The current results support our previous findings showing that removal of the N-terminal extension of rβA3-crystallin increased the binding affinity for dimer formation (*23*). Extending these studies to βB2-crystallin, we show here that removal of the N-terminal extension has little effect, and removal of N- and C-terminal extensions, results in modest increases in the binding affinity for this protein. This demonstrates that the effects of the terminal arms on rβA3 and rβB2 association vary depending on the specific crystallin and the sequence of the terminal extension. These studies on the energetics of dimerization cannot provide information on the rates of subunit exchange. We have only rough estimates for this rate, derived from formation of βA3- and βB2-heterodimers from their respective homodimers (*24*).

The fraction of dimer α at 10 μM concentration as a function of the temperature was calculated using the K_d data from Tables 2 and 3 and is shown in Figure 3C. Truncated crystallin rβA3Ntr has a higher propensity to dimerize compared to rβB2Ntr, rβB2NCtr, and wild-type proteins. The dimer fractions α of both wild type (rβA3) and truncated (rβA3Ntr) crystallins clearly increase with temperature and this trend is seen to a lesser extent with the wild type and truncated forms of rβB2. However, in the eye lens, which has protein concentration greater than 300 mg/mL, the great majority of all β-crystallins would be expected to be associated, which might contribute to the decreased light scattering seen at these high protein concentrations (*41*). In addition, interactions with other crystallins to form heterodimers, which may be somewhat favored over homodimers, and higher order associates would tend to shift the equilibrium toward association.

Domain−Domain Interactions. Interactions between protein domains are important for dimer stabilization. Measurement of dimer formation at different temperatures has allowed dissection of the binding free energy into contributions from changes in both enthalpy and entropy (Table 4). For both, rβA3 and rβB2, negative values of ΔG_a derive from positive values of both enthalpy ΔH_a and entropy ΔS_a, indicating that protein association is entropically driven ($-T\Delta S_a < 0$ while $\Delta H_a > 0$), which is similar to that of found for tubulin dimerization (*42*, *43*). Experimentally, this is seen as dimerization increasing with temperature (Figure 4). The truncated proteins rβA3Ntr, rβB2Ntr, and rβB2NCtr all contain the basic two-domain structure common to $\beta\gamma$-crystallins (Figure 1). However, rβA3Ntr forms a more stable dimer despite larger positive ΔH_a values. Moreover, over the temperature range 5−20 °C, rβA3Ntr and rβB2NCtr have higher dimerization potentials than the wild-type proteins. Interestingly, mutant rβA3Ntr forms the tightest dimer among all the crystallins examined (Table 1).

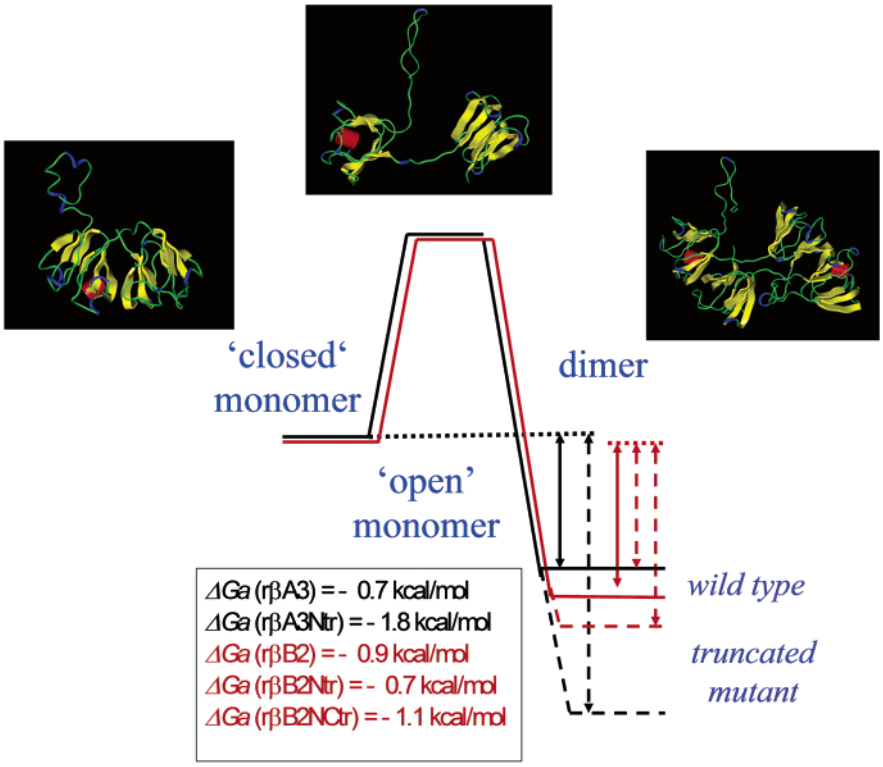

FIGURE 4: Schematic representation of rβA3 monomer and dimer structures coexisting in equilibrium in solution. (Top) Structures of monomer forms and dimer were predicted using homology modeling (*23*). Monomer and dimer forms coexist in rapid equilibrium in solution over a wide temperature range in the absence of higher order oligomers and aggregates. The connecting N- and C-terminal domains interdomain loop adopt two possible conformations either folded for the "closed" form of the monomer or extended for the "opened" form of the monomer and dimer; (bottom) diagram representing Gibbs free energy changes for the monomer−dimer equilibrium is indicated by solid black (rβA3), broken black (rβA3Ntr), solid red (rβB2), and broken red (rβB2Ntr and rβB2NCtr) lines. Values of free energy changes at 20 °C were taken from Tables 2 and 3 and are indicated by arrows. This figure does not imply that the initial energies of βA3- and βB2-crystallin and their variants are equal.

Terminal Extensions. β-Crystallin terminal arms have also been suggested to have an independent role in further association of dimers into both higher order associates and interactions with other cellular components (*32*). Thus, while loss of the terminal extensions appears to favor reversible dimer formation, the effects on formation of higher order associates is hard to predict. As an example, both βA3- and βB1-crystallin, which has the longest N-terminal extension, are found in larger aggregates β-crystallin (*44*, *45*). The situation is also complicated by the tendency of β-crystallin terminal arms to be truncated with age. Although the loss of terminal extensions during lens fiber aging is well-known and has been investigated in some forms of cataracts (*46*), which crystallins are most affected by this process and the extent to which it occurs is still debated. For example, mass spectrometry of insoluble protein from the human lens identified N-terminal truncated βB1 and βA3/βA1 crystallins (*47*). Similarly, truncated forms of βA3-crystallin were found in lens proteins of aging mice (*48*) and in the soluble protein of young rat (*49*) lenses. Furthermore, age-dependent cleavage of the C-terminal extension of bovine βB2-crystallin (*50*) and at the N-terminal extensions of βA3- or βB2-crystallins have been reported (*29*, *30*, *51*−*54*). Terminal extensions are proteolytically processed by thiol proteases (*52*, *53*). Computational modeling from these data suggests that rather than recognizing specific sequence sites, at least some thiol proteases appear to recognize accessible sites at positions separated by more protected microdomains of 5−10 amino acids (*55*).

One potential difficulty with the above analysis is that it is, in part, based on modeled structures for the different β-crystallins. Molecular modeling of βA3-crystallin based on the known crystallographic structures of γB- and βB2-crystallin seems reasonable based on the known conserved domain structures of all $\beta\gamma$-crystallins studied to date (*4*, *56*), the structural similarities of βA3- and βB2-crystaliins based on circular dichroism studies (*24*), and the ability of all β-crystallins to interact to form both homo- and heterodimers and higher order aggregates (*57*). However, the crystal structure is not known, and analyses based on molecular modeling require some caution due to potential inaccuracies in the predicted structure.

The results presented here on the energetics of monomer−dimer equilibrium allow us to speculate on the structural and functional role of the terminal extensions. For instance, in dimer formation, the removal of the terminal extensions of rβA3 and rβB2 results in increases in both enthalpy (+10.9 and +7.0 kcal/mol, respectively) and entropy (+40.7 and +23.4 e.u.). As the N- and C-terminal extensions are largely unstructured and highly mobile (*9*, *26*, *58*), a significant portion of the overall entropy change could be derived from rotational and translational movements of the molecule (*23*). This effect may be more pronounced for β-crystallins with longer extensions such as in βA3-crystallin, and perhaps βB1-crystallin. Therefore, terminal extensions possibly reduce the rβA3 and rβB2 propensities to associate into dimers, or higher oligomers, by decreasing the rotational and translational freedom (entropy) of the molecule.

Truncated crystallins (rβA3Ntr and rβB2NCtr) show a higher propensity to dimerize compared to wild-type proteins (Figure 3C). This may favor formation of higher molecular weight associates as truncated β-crystallins accumulate during aging or normal development. We recently demonstrated that rβA3Ntr has increased sensitivity to UV-light induced photoaggregation (manuscript in preparation). This suggests that the age-related cleavage of N-terminal extension of βA3 crystallin might increase susceptibility to insoluble protein formation and thus cataract formation.

ACKNOWLEDGMENT

The authors are very grateful to Dr. Hassan Mchaorab (Vanderbilt University) for providing a clone of βB2 crystallin, and Dr. Samuel Zigler (NEI, NIH) for kindly providing polyclonal βB2-crystallin antibody. The authors also are thankful to the Center of Molecular Modeling at National Institutes of Health for using commercial molecular modeling software on network.

REFERENCES

1. Wistow, G. J., and Piatigorsky, J. (1988) *Annu. Rev. Biochem. 57*, 479−504.
2. Bloemendal, H., and de Jong, W. W. (1991) *Prog. Nucleic Acid. Res. Mol. Biol. 41*, 259−281.
3. Caspers, G. J., Leunissen, J. A., and de Jong, W. W. (1995) *J. Mol. Evol. 40*, 238−248.
4. Lubsen, N. H., Aarts, H. J. M., and Schoenmakers, J. G. G. (1988) *Prog. Biophys. Mol. Biol. 51*, 47−76.
5. Wistow, G., Turnell, B., Summers, L., Slingsby, C., Moss, D., Miller, L., Lindley, P., and Blundell, T. (1983) *J. Mol. Biol. 170*, 175−202.
6. Sergeev, Y. V., Chirgadze, Y. N., Mylvaganam, S. E., Driessen, H., Slingsby, C., and Blundell, T. L. (1988) *Proteins 4*, 137−147.
7. White, H. E., Driessen, H. P. C., Slingsby, C., Moss, D. S., and Lindley, P. F. (1989) *J. Mol. Biol. 207*, 217−235.
8. Bax, B., Lapatto, R., Nalini, V., Driessen, H., Lindley, P. F., Mahadevan, D., Blundell, T. L., and Slingsby, C. (1990) *Nature 347*, 776−780.
9. Lapatto, R., Nalini, V., Bax, B., Driessen, H., Lindley, P. F., Blundell, T. L., and Slingsby, C. (1991) *J. Mol. Biol. 222*, 1067−1083.
10. Chambers, C., and Russell, P. (1991) *J. Biol. Chem. 266*, 6742−6746.
11. Cartier, M., Breitman, M. L., and Tsui, L. C. (1992) *Nat. Genet. 2*, 42−45.
12. Litt, M., Carrero-Valenzuela, R., LaMorticella, D. M., Schultz, D. W., Mitchell, T. N., Kramer, P., and Maumenee, I. H. (1997) *Hum. Mol. Genet. 6*, 665−668.
13. Klopp, N., Favor, J., Loster, J., Lutz, R. B., Neuhauser-Klaus, A., Prescott, A., Pretsch, W., Quinlan, R. A., Sandilands, A., Vrensen, G. F., and Graw, J. (1998) *Genomics 52*, 152−158.
14. Kannabiran, C., Rogan, P. K., Olmos, L., Basti, S., Rao, G. N., Kaiser-Kupfer, M., and Hejtmancik, J. F. (1998) *Mol. Vision 4*, 21.
15. Graw, J. (1999) *Prog. Retinal Eye Res. 18*, 235−267.
16. Heon, E., Priston, M., Schorderet, D. F., Billingsley, G. D., Girard, P. O., Lubsen, N., and Munier, F. L. (1999) *Am. J. Hum. Genet. 65*, 1261−1267.
17. Ren, Z., Li, A., Shastry, B. S., Padma, T., Ayyagari, R., Scott, M. H., Parks, M. M., Kaiser-Kupfer, M., and Hejtmancik, J. F. (2000) *Hum. Genet. 106*, 531−537.
18. Stephan, D. A., Gillanders, E., Vanderveen, D., Freas-Lutz, D., Wistow, G., Baxevanis, A. D., Robbins, C. M., VanAuken, A., Quesenberry, M. I., Bailey-Wilson, J., Juo, S. H., Trent, J. M., Smith, L., and Brownstein, M. J. (1999) *Proc. Natl. Acad. Sci. U.S.A. 96*, 1008−1012.
19. Kmoch, S., Brynda, J., Asfaw, B., Bezouska, K., Novak, P., Rezacova, P., Ondrova, L., Filipec, M., Sedlacek, J., and Elleder, M. (2000) *Hum. Mol. Genet. 9*, 1779−1786.
20. Mayr, E. M., Jaenicke, R., and Glockshuber, R. (1994) *J. Mol. Biol. 235*, 84−88.
21. Bax, B., and Slingsby, C. (1989) *J. Mol. Biol. 208*, 715−717.
22. Sergeev, Y. V., and Hejtmancik, J. F. (1997) in *Techniques in Protein Chemistry* (Marshak, D. R., Ed.) pp 817−826, Academic Press, New York.
23. Sergeev, Y. V., Wingfield, P. T., and Hejtmancik, J. F. (2000) *Biochemistry 39*, 15799−15806.
24. Hejtmancik, J. F., Wingfield, P., Chambers, C., Russell, P., Chen, H.-C., Sergeev, Y. V., and Hope, J. N. (1997) *Protein. Eng. 10*, 1347−1352.
25. Norledge, B. V., Mayr, E. M., Glockshuber, R., Bateman, O. A., Slingsby, C., Jaenicke, R., and Driessen, H. P. (1996) *Nat. Struct. Biol. 3*, 267−274.
26. Werten, P. J. L., Carver, J. A., Jaenicke, R., and de Jong, W. W. (1996) *Protein Eng. 9*, 1021−1028.
27. Werten, P. J., Lindner, R. A., Carver, J. A., and de Jong, W. W. (1999) *Biochim. Biophys. Acta 1432*, 286−292.
28. Kroone, R. C., Elliott, G. S., Ferszt, A., Slingsby, C., Lubsen, N. H., and Schoenmakers, J. G. G. (1994) *Protein Eng. 7*, 1395−1399.
29. Hope, J. N., Chen, H.-C., and Hejtmancik, J. F. (1994) *J. Biol. Chem. 269*, 21141−21145.
30. Hope, J. N., Chen, H. C., and Hejtmancik, J. F. (1994) *Protein Eng. 7*, 445−451.
31. Hope, J. N., Chambers, C., Rusell, P., Lee, L., and Hejtmancik, J. F. (1996) Function of N-terminal extension in beta-B2-crystallin. *Invest. Ophthalmol. Visual Sci. 36*, s886, Abstract.
32. Trinkl, S., Glockshuber, R., and Jaenicke, R. (1994) *Protein Sci. 3*, 1392−1400.
33. Laemmli, U. K. (1970) *Nature 227*, 680−685.
34. Towbin, H., Staehelin, T., and Gordon, J. (1979) *Proc. Natl. Acad. Sci. U.S.A. 76*, 4350−4354.
35. Cole, J. L., and Hansen, J. C. (1999) *J. Biomol. Tech. 10*, 163−176.
36. Laue, T. M., Shah, B. D., Ridgeway, T. M., and Pelletier, S. L. (1992) in *Analytical Ultracentrifugation in Biochemistry and Polymer Science* (Harding, S. E., Rowe, A. J., and Horton, J. C., Eds.) pp 90−125, Royal Society for Chemistry, Cambridge, United Kingdom.
37. Sakurai, K., Oobatake, M., and Goto, Y. (2001) *Protein Sci. 10*, 2325−2335.
38. Lampi, K. J., Oxford, J. T., Bachinger, H. P., Shearer, T. R., David, L. L., and Kapfer, D. M. (2001) *Exp. Eye Res. 72*, 279−288.
39. Bateman, O. A., Lubsen, N. H., and Slingsby, C. (2001) *Exp. Eye Res. 73*, 321−331.
40. Correia, J. J., Chacko, B. M., Lam, S. S., and Lin, K. (2001) *Biochemistry 40*, 1473−1482.
41. Delaye, M., and Tardieu, A. (1983) *Nature 302*, 415−417.
42. Sackett D. L., Lippoldt, R. (1991) *Biochemistry 30*, 3511−3517.
43. Ross P. D., Subramanian, S. (1981) *Biochemistry 20*, 3096−3102.
44. Vermorken, F. J. M., Herbrink, P., and Bloemendal, H. (1977) *Eur. J. Biochem. 78*, 617−622.
45. Ajaz, M. S., Ma, Z., Smith, D. L., and Smith, J. B. (1997) *J. Biol. Chem. 272*, 11250−11255.
46. Shearer, T. R., Ma, H., Fukiage, C., and Azuma, M. (1997) *Mol. Vision 3*, 8.
47. Hanson, S. R., Hasan, A., Smith, D. L., and Smith, J. B. (2000) *Exp. Eye Res. 71*, 195−207.
48. Ueda, Y., Duncan, M. K., and David, L. L. (2002) *Invest. Ophthalmol. Vision Sci. 43*, 205−215.
49. Lampi, K. J., Shih, M., Ueda, Y., Shearer, T. R., and David, L. L. (2002) *Invest. Ophthalmol. Vision Sci. 43*, 216−224.
50. Takemoto, L. (1995) *Exp. Eye Res. 61*, 743−748.
51. Takemoto, L., Takemoto, D., Brown, G., Takehana, M., Smith, J., and Horwitz, J. (1987) *Exp. Eye Res. 45*, 385−392.
52. David, L. L., Shearer, T. R., and Shih, M. (1993) *J. Biol. Chem. 268*, 1937−1940.
53. David, L. L., and Shearer, T. R. (1993) *FEBS Lett. 324*, 265−270.
54. David, L. L., Azuma, M., and Shearer, T. R. (1994) *Invest. Ophthalmol. Vision Sci. 35*, 785−793.
55. Sergeev, Y. V., David, L. L., Chen, H.-C., Hope, J. N., and Hejtmancik, J. F. (1998) *Mol. Vision 4*, 9.
56. Slingsby, C., and Clout, N. J. (1999) *Eye 13*, 395−402.

57. Bloemendal, H. (1981) *Molecular and Cellular Biology of the Eye Lens* Wiley, New York.
58. Carver, J. A., Cooper, P. G., and Truscott, R. J. (1993) *Eur. J. Biochem. 213*, 313−320.
59. Cohn, E. J., and Edsall, J. T. (1943) *Proteins, Amino Acids and Peptides* Van Nostrand-Reinhold, Princeton, NJ.

BI034617F